

1 Title page

2

3 **Title**

4 **An ancestral apical brain region contributes to the central complex under the control of *foxQ2* in the**
5 **beetle *Tribolium castaneum***

6

7 **Running title**

8 *foxQ2* in central complex development

9

10 **Authors**

11 Bicheng He¹

12 Marita Buescher¹

13 Max Stephen Farnworth^{1/2}

14 Frederic Strobl³

15 Ernst Stelzer³

16 Nikolaus Dieter Bernhard Koniszewski¹

17 Dominik Mühlen¹

18 Gregor Bucher¹

19

20 ¹ Johann Friedrich Blumenbach Institute of Zoology, GZMB, University of Goettingen

21 Justus-von-Liebig-Weg 11

22 37077 Göttingen

23

24 ² Göttingen Graduate Center for Molecular Biosciences, Neurosciences and Biophysics,

25 Göttingen, Germany

26

27 ³ Buchmann Institute for Molecular Life Sciences (BMLS), Goethe University – Frankfurt am Main

28 Max-von-Laue-Straße 15, Frankfurt am Main D-60438, Germany

29

30

31 Mail of corresponding author:

32 gbucher1@uni-goettingen.de

33

34

35 **Key words**

36 *foxQ2*, TC004761, central complex, protocerebrum, commissure, apical organ, *Tribolium*

37 *castaneum*, *fd102*, CG11152

38

39 [Summary statement](#)

40 An ancestral neuroendocrine center contributes to the evolution of the central complex. *foxQ2* is a gene
41 required for the development of midline structures of the insect brain, which distinguish protocerebrum
42 from segmental ganglia.

43

44 [Abstract](#)

45 The genetic control of anterior brain development is highly conserved throughout animals. For instance,
46 a conserved anterior gene regulatory network specifies the ancestral neuroendocrine center of animals
47 and the apical organ of marine organisms. However, its contribution to the brain in non-marine animals
48 has remained elusive. Here, we study the function of the *Tc-foxQ2* forkhead transcription factor, a key
49 regulator of the anterior gene regulatory network of insects. We characterized four distinct types of *Tc-*
50 *foxQ2* positive neural progenitor cells based on differential co-expression with *Tc-six3/optix*, *Tc-six4*, *Tc-*
51 *chx/vsx*, *Tc-nkx2.1/scro*, *Tc-ey*, *Tc-rx* and *Tc-fez1*. An enhancer trap line built by genome editing marked
52 *Tc-foxQ2* positive neurons, which projected through the primary brain commissure and later through a
53 subset of commissural fascicles. Eventually, they contributed to the central complex. Strikingly, in *Tc-*
54 *foxQ2* RNAi knock-down embryos the primary brain commissure did not split and subsequent
55 development of midline brain structures stalled. Our work establishes *foxQ2* as a key regulator of brain
56 midline structures, which distinguish the protocerebrum from segmental ganglia. Unexpectedly, our data
57 suggest that the central complex evolved by integrating neural cells from an ancestral anterior
58 neuroendocrine center.

59

60 Introduction

61 The brain is among the most complex organs found in animals. During development many different types
62 of neurons are specified to build the macrocircuitry of the central nervous system before the
63 microcircuitry is established. Understanding the genetic and cellular underpinnings of brain development
64 has remained one of the major challenges in developmental biology. Many aspects of neural
65 development are conserved in animals but compared to vertebrates, insects have a strongly reduced
66 number of neural cells and the genes involved are usually present in single copy. This has made insects
67 very useful models to study the genetic control of neural development (Hartenstein and Stollewerk,
68 2015; Technau et al., 2006). The insect central nervous system is composed of serially homologous
69 segmental ganglia (Snodgrass, 1935; Weber, 1966). However, the anterior-most part of the brain, the
70 protocerebrum, is of different origin. It stems from an anterior non-segmental tissue dating back to the
71 last common bilaterian ancestor (Arendt et al., 2008; Rempel, 1975; Scholtz and Edgecombe, 2006;
72 Snodgrass, 1935; Strausfeld, 2012; Weber, 1966). Accordingly, a number of neural patterning genes are
73 expressed in the anterior brain anlagen but not in the trunk of animals from vertebrates to insects
74 (Acampora et al., 1998; Arendt and Nübler-Jung, 1996; Arendt et al., 2008; Gehring, 1996; Hirth et al.,
75 1995; Hirth et al., 2003; Lowe et al., 2003; Posnien et al., 2011b; Qiring et al., 1994; Sinigaglia et al.,
76 2013; Steinmetz et al., 2010). Conversely, a number of transcription factors that confer spatial identity to
77 trunk neuroblasts (NBs) are expressed in a quite modified way or not at all in the protocerebral
78 neuroectoderm (Urbach and Technau, 2003a; Urbach and Technau, 2003b). A number of profound
79 structural differences distinguish the protocerebrum from segmental ganglia. The former contains
80 unique structures like the optic lobes, the mushroom bodies and is marked by a set of midline-spanning
81 neuropils, the central complex (CX) (El Jundi and Heinze, 2016; Pfeiffer and Homberg, 2014; Snodgrass,
82 1935; Strausfeld, 2012; Weber, 1966). Further, the protocerebral commissures develop in a different
83 way. In each trunk segment, two commissures connect the hemi-ganglia but their axons do not switch
84 between the two commissures. The primary protocerebral commissure, by contrast, grows much larger
85 and splits into a number of commissural fascicles connecting the brain lobes. Fascicle switching of
86 neurites between these fascicles does occur and is essential for CX development (Boyan et al., 2008;
87 Boyan et al., 2017).

88 Recently, a molecular subdivision within the protocerebrum was found where an anterior *optix/six3*
89 positive region distinguishes an ancestral neuroendocrine center of animals from a more posterior
90 *otd/otx* positive region (Kittelman et al., 2013; Steinmetz et al., 2010). The components and some of
91 their interactions of the anterior gene regulatory network (aGRN) including *six3* and *foxQ2* are conserved
92 within animals (Hunnekuhl and Akam, 2014; Kitzmann et al., 2017; Lowe et al., 2003; Marlow et al.,
93 2013; Range and Wei, 2016; Sinigaglia et al., 2013; Wei et al., 2009; Yaguchi et al., 2008; Yaguchi et al.,
94 2010). Apart from marking neuroendocrine cells throughout animal clades, this neural region gives rise
95 to the apical organ of marine animals including ciliated cells like the apical tuft (Dunn et al., 2007;
96 Marlow et al., 2013; Santagata et al., 2012; Sinigaglia et al., 2013; Wei et al., 2009). However, it has
97 remained unclear to what non-neuroendocrine structures this region might contribute in arthropods,
98 which do not have an apical organ (Hunnekuhl and Akam, 2014; Marlow et al., 2014).

99 Unfortunately, central brain development is quite derived in the main model for insect genetics,
100 *Drosophila melanogaster*. Hence, we have been using the red flour beetle *Tribolium castaneum* as
101 complementary model system. First, it represents a more ancestral situation of anterior neuroectoderm
102 development contrasting the quite derived situation with respect to location, geometry and genetic
103 control of the head and neuroectoderm anlagen in *Drosophila* (Kittelman et al., 2013; Posnien et al.,

104 2010). Second, a functional CX forms at least partially during embryogenesis (Koniszewski et al., 2016;
105 Panov, 1959; Wegerhoff and Breidbach, 1992) while in *Drosophila* the first functional CX appears during
106 pupation. Hence, both embryonic spatial signals and outcome of protocerebrum development are
107 reflected in a more typical way in the *Tribolium* embryo compared to *Drosophila*. With respect to
108 transgenesis, misexpression, genome editing, efficient genome wide RNAi screening and other tools for
109 analysis of gene function, *Tribolium* is a genetic model insect second only to *Drosophila* (Berghammer et
110 al., 1999; Bucher et al., 2002; Dönitz et al., 2018; Gilles et al., 2015; Schinko et al., 2010; Schmitt-Engel et
111 al., 2015; Tomoyasu and Denell, 2004; Trauner et al., 2009).

112 In this work we asked for the role of the forkhead transcription factor *Tc-foxQ2* in brain development
113 because this gene is exclusively expressed in the region patterned by the aGRN (Kitzmann et al., 2017).
114 Further, it is a highly conserved anterior patterning gene. Orthologs of *foxQ2* are involved in anterior-
115 most specification of neural cells in many clades of bilaterians and in cnidarians (Darras et al., 2011;
116 Fritzenwanker et al., 2014; Hunnekuhl and Akam, 2014; Leclère et al., 2016; Marlow et al., 2013; Range
117 and Wei, 2016; Range and Wei, 2016; Sinigaglia et al., 2013; Wei et al., 2009; Yaguchi et al., 2008;
118 Yaguchi et al., 2010; Yu et al., 2003). A notable exception are amphibians and mammals, where the gene
119 was lost from the genome (Mazet et al., 2003). In arthropods, anterior expression of *foxQ2* orthologs
120 was described in *Drosophila* (*fd102C*, CG11152) and *Strigamia maritima*, a myriapod (Hunnekuhl and
121 Akam, 2014; Lee and Frasch, 2004) correlating with the location of neuroendocrine cells. Recently, we
122 have shown an upstream role of *Tc-foxQ2* in anterior head epidermis patterning in *Tribolium* where it
123 acts together with *six3/optix* upstream in the aGRN to build the labrum (Kitzmann et al., 2017). A
124 modification of the shape of the central body (CB) was noted in that work but apart from that, functional
125 data on the neural function of *foxQ2* is badly missing in any protostome.

126 We found that *Tc-foxQ2* was continuously expressed in anterior median cell clusters from neural
127 progenitors to postmitotic neurons of the late embryonic, larval and adult brains. Based on co-
128 expression with other protocerebral patterning genes we characterized four different types of *Tc-foxQ2*
129 positive neural progenitor cells. Further, we generated genetic neural imaging lines and found that *Tc-*
130 *foxQ2* positive neurons project through the primary brain commissure and later into the upper unit of
131 the central body (fan-shaped body). *Tc-foxQ2* RNAi-knock-down embryos failed to develop brain midline
132 structures: The primary brain commissure did form but failed to split into the large number of
133 protocerebral commissures. Consequently, the CB formation was abolished. These results identify *Tc-*
134 *foxQ2* as one of the key factors of embryonic brain development contributing to the different
135 development of the protocerebrum versus segmental ganglia. Unexpectedly, our results show that cells
136 patterned by the aGRN contribute to the CX, a unique protocerebral brain structure. Apparently, the
137 insect CX evolved by integrating cells from the ancestral anterior-most neuroectoderm, which gives rise
138 to the apical organ including the apical tuft in marine animals.

139

140

141

142 Results

143 *Tc-foxQ2* marks neural progenitor cells with four different molecular identities

144 In the embryo, *Tc-foxQ2* is expressed in the anterior neuroectoderm from earliest stages onwards
145 indicating a role in the specification of neuroblasts (Kitzmann et al., 2017). Hence, we sought to
146 determine which neural progenitor cells (NPCs) expressed *Tc-foxQ2*. To that end we generated an
147 antibody specific for the Tc-FoxQ2 protein (see Supplementary materials and methods; Fig. S1) and used
148 an intronic probe of *Tc-asense* (*Tc-ase*) as marker for NPCs, which could be either NBs (Wheeler et al.,
149 2003), intermediate neural progenitors (INPs) of type II NBs or ganglion mother cells (GMCs) (Boone and
150 Doe, 2008; Bowman et al., 2008). In addition, size and cell shape together with large nuclei were used to
151 recognize progenitor cells. See Fig. S2 for staging (Biffar and Stollewerk, 2014) and for the comparison of
152 the signals of exonic and intronic *Tc-ase* probes.

153 The first protocerebral NPCs delaminate at NS4. The first Tc-FoxQ2⁺ NPCs, however, emerge at NS8.
154 Here, about 15 *Tc-foxQ2*⁺/*Tc-ase*⁺ cells were identified (n=6; Fig. 1A; Table S1) forming a large anterior
155 group (blue and green in Fig. 1A''), a small median group (gray) and a single lateral cell (orange). These
156 groups correspond to three domains into which the *Tc-foxQ2* expression splits in the neuroectoderm
157 (Kitzmann et al., 2017). At NS11, the number had decreased to 9-12 cells expressing both markers (n=6;
158 Fig. 1B; Table S1) while at least 5-7 cells were observed at stage 14 (n=6; Fig. 1C; Table S1). This reduction
159 could have several reasons: *Tc-ase* expression may cease once NBs enter quiescence like in *Drosophila*
160 (Lai and Doe, 2014) or *Tc-foxQ2* expression may become repressed in a subset of NPCs. Alternatively, if
161 the anterior group contained type II NBs, the double positive cells would be INPs or GMCs, which based
162 on *Drosophila* knowledge express *asense* while type II NBs themselves do not (Boone and Doe, 2008;
163 Bowman et al., 2008). Unfortunately, there are currently no established markers for unequivocally
164 distinguishing NBs, INPs and GMCs in *Tribolium*.

165 The identity of NPCs is believed to be determined by unique cocktails of transcription factors (Skeath,
166 1999; Urbach and Technau, 2003a). In order to check whether the positional groups were also
167 molecularly distinct we performed co-expression analyses (n=6 embryos). We used a number of almost
168 exclusive anterior patterning genes because these were likely to contribute to protocerebrum specific
169 patterning (Posnien et al., 2011a; Posnien et al., 2011b; Steinmetz et al., 2010), the co-expression of
170 which we were able to follow until stage NS11 when morphogenetic movements and the increase in cell
171 number made an identification of individually marked cells challenging. We found four different
172 molecular types that correlated with positional differences (Fig. 2). The first type (No1 in Fig. 2I') was the
173 largest group and was located anterior median in the neuroectoderm. This type showed co-expression of
174 *Tc-foxQ2* with *Tc-six3* (*optix*), *Tc-six4* and later *Tc-chx* (*vsx*). We call these cells the *P-fox-am* group of cells
175 (P stands for protocerebral according to *Drosophila* nomenclature (Younossi-Hartenstein et al., 1996)).
176 The second type (*P-fox-amp*) was located posteriorly adjacent and was similar to the *P-fox-am* but
177 showed additional expression of *Tc-scro* (*nkx2.1*), *Tc-earmuff* (*fez1*) and in one of the cells also *Tc-eyeless*
178 (*Pax6*) (No2 in Fig. 2I'). A third type consisted of one lateral NPC, which co-expressed *Tc-six3* with *Tc-*
179 *earmuff*, *Tc-rx* and *Tc-eyeless* (No3 in Fig. 2I'). Due to its separate location and molecular distinction, this
180 cell type (*P-fox-l*) could be followed through several stages (orange in Fig. 1). The fourth type showed
181 only co-expression of *Tc-foxQ2* and *Tc-scro* (No4 in Fig. 2I') and was located at a ventral position adjacent
182 to the stomodeum (*P-fox-v*).

183 We were not able to homologize these NPCs with those of *Drosophila* or *Tenebrio*. This was due to the
184 lack of a comprehensive map of all brain NBs in *Tribolium*, lack of data for most of the respective

185 expression patterns in *Drosophila* NBs and the morphological differences between *Tribolium* and both
186 *Drosophila* and *Tenebrio* (Urbach and Technau, 2003a; Urbach et al., 2003). However, based on the
187 exclusively pre-antennal expression of *Tc-foxQ2* during embryogenesis (Kitzmann et al., 2017), we assign
188 all cells to the protocerebrum. We found no *Tc-FoxQ2*⁺ cells in the more posterior parts of the brain or
189 the ventral nerve cord.

190 Taken together, our analysis showed that *Tc-foxQ2* marks four distinct types of *Tc-ase* positive cells in
191 the early neuroectoderm. Its expression suggests a role in the specification of NPCs in the protocerebral
192 part of the insect brain.

193 Marking of the genetic *Tc-FoxQ2* neural lineage by a CRISPR/Cas9 induced enhancer trap

194 Orthologs of *foxQ2* are involved in anterior-most patterning in animals including development of the
195 apical organ (Marlow et al., 2014; Sinigaglia et al., 2013; Yaguchi et al., 2010). In insects, *foxQ2* is
196 exclusively expressed in protocerebral tissue and a function in protocerebrum-specific neuropils has
197 been suggested (Kitzmann et al., 2017). However, *foxQ2*⁺ neurons had not been marked to follow their
198 projections in any insect. Unfortunately, *foxQ2* enhancer trap lines were neither available for *Tribolium*
199 nor *Drosophila*. Hence, we used CRISPR/Cas9 genome editing (Gilles et al., 2015) for a non-homologous
200 end joining strategy to generate an enhancer trap in the *Tc-foxQ2* locus that drives EGFP (see
201 Supplementary materials and methods; Table S2- S4; Fig S3, Farnworth et al. in press). By double
202 immunohistochemistry we confirmed that EGFP and *Tc-FoxQ2* protein expression correlated quite well
203 throughout embryogenesis (Fig. 3). The observed differences appeared to be mainly due to different
204 dynamics of maturation and degradation of the two proteins but we cannot exclude that cells are single
205 positive for either EGFP or *Tc-FoxQ2*. We called this line *foxQ2-5'-line* and used it for all subsequent
206 analyses of *Tc-foxQ2*⁺ neurons.

207 During embryogenesis from NS3 to NS13, the *Tc-FoxQ2* antibody and EGFP stainings closely matched the
208 in situ hybridization patterns (Kitzmann et al., 2017). Essentially, *Tc-FoxQ2* was initially expressed in two
209 bilateral anterior-median expression domains (Fig. 3A). Later, these resolved into a stomodeal (asterisk
210 in Fig. 3B' and F') and an anterior domain, which was further subdivided into a median (white
211 arrowhead) and lateral domain (open arrowhead). The *P-fox-v* NPCs were located in the stomodeal
212 domain while the other types emerged from within the anterior domains. Towards the end of
213 embryogenesis (NS15) two clusters of cells reminiscent of neural lineages were observed: A large
214 anterior median group (white arrowhead in Fig. 3F') and a smaller lateral group (open arrowhead). In
215 addition, scattered cells were observed more posteriorly in the brain and strong staining in the
216 stomodeum persisted (asterisk).

217 Three *Tc-FoxQ2* positive cell clusters contribute to brain midline structures including the central 218 body

219 We characterized the contribution of *Tc-foxQ2*⁺ cells to the embryonic brain. We found no *Tc-foxQ2*⁺ glia
220 based on immunohistochemistry in our transgenic glia reporter line *glia-blue* (Koniszewski et al., 2016)
221 (not shown). In order to study the development of the projection patterns of *Tc-foxQ2*⁺ neurons we
222 performed double-immunohistochemistry visualizing the EGFP derived from the *foxQ2-5'-line* combined
223 with β -acetylated tubulin (acTub), which marks axonal projections (Piperno and Fuller, 1985). We
224 detected at least three clusters of *Tc-foxQ2*⁺ cells with properties of neural lineages (Fig. 4, please find
225 entire stacks and videos on figshare).

226 At stage NS13, the first brain commissure became visible in the acTub staining (white arrowhead in Fig.
227 4A'). One large continuous cluster of about 89 *Tc-foxQ2*⁺ cells was situated around this primary
228 commissure and was located in the anterior median part of the forming brain (n=5; Fig. 4A; Table S5).
229 About 12 marked cells had the nuclear morphology of NPCs (n=5; Fig. 4A; Table S5). We termed this
230 group of adjacent cells the *anterior-median-foxQ2-cluster*. Based on the number of observed NPCs within
231 the cluster and the number of projections that emerge from it we assume that it could be composed of
232 several neural lineages. During subsequent development, these cells stayed together but along with
233 general morphogenetic movements they approached each other towards the midline (compare distance
234 in Fig. 4B with E; see Supplementary movie 1 and 2).

235 At NS 14 the cell number in the *anterior-median-foxQ2-cluster* had increased to about 150 (n=5; Fig. 4B;
236 Table S5) and 14 *Tc-FoxQ2*⁺ NPCs were still discernable (e.g. hatched circle in Fig. 4B'). At that stage, the
237 first EGFP positive projections became visible. They projected towards the brain commissure and joined
238 it. However, at that stage, the EGFP⁺ projections had not yet reached the midline of the commissure
239 (white arrowhead in Fig. 4B).

240 By NS15 the cell number of the *anterior-median-foxQ2-cluster* had increased to approximately 210-240
241 cells (n=5; Fig. 4C-E; Table S5) but NPCs were no longer distinguishable by morphological means. The
242 brain commissure had split and expanded significantly by additional projections from other lineages (Fig.
243 4C'-E'). Likewise, the projections of the *anterior-median-foxQ2-cluster* became more complex. About 6-7
244 axon bundles emanated from that cluster to separately join the central brain primordium (arrow in Fig.
245 4C') to cross the midline. EGFP signal distinguished at least three major sites of midline structures with
246 *Tc-foxQ2*⁺ contribution: One in the half-ring-like circumesophageal commissure (white arrowhead in Fig.
247 4E), and two separate fascicles within the central brain primordium (white arrowheads in Fig. 4D).
248 Intriguingly (arrowheads in Fig. 4D').

249 In order to assign the *anterior-median-foxQ2-cluster* to characterized NPCs we traced back the EGFP
250 signal from NS15 to the embryonic neuroectoderm. Based on continuous expression from NS3 to NS15
251 and in vivo imaging data on its development (Supplementary movie 1 and 2) we suggest that it is derived
252 from *P-fox-am* type of NPCs. By crossing with the transgenic glia marker line *glia-red* (Koniszewski et al.,
253 2016) we found that most cells of the cluster were surrounded by one glial sheet indicating that they
254 formed one large neural lineage (white arrowhead in Fig. S4). A second glia sheet appeared to surround
255 the medial-most cells marked with lower levels of EGFP (open arrowhead in Fig. S4).

256 A second group of EGFP positive cells emerged laterally to that cluster after NS13 (*anterior-lateral-*
257 *foxQ2-lineage*). At NS 14 one NPC and a very small group of cells (6-8) were marked by EGFP (n=4;
258 orange arrowhead in Fig. 5A; Table S6). At NS15 approximately 15-20 cells were marked (n=4; Table S6).
259 They formed a column-like cluster lateral to the *anterior-median-foxQ2-cluster* (orange arrowheads in
260 Fig. 5B, D) and their projections joined the established *Tc-foxQ2* positive neurites at a lateral position
261 (white arrows in Fig. 5B, D). Because this cluster contained only one NB and all cells were within one glia
262 sheath (orange arrowhead in Fig. S4) we hypothesize that they form one neural lineage. By tracing back
263 this lineage to the embryonic ectoderm we found that it most likely derived from the *P-fox-I* NPC (Fig.
264 2I').

265 The lineages of anterior median NBs are known to contribute to the CX (Boone and Doe, 2008; Bowman
266 et al., 2008; Boyan et al., 2010; Walsh and Doe, 2017). We showed that some NPCs are *Tc-foxQ2* positive
267 and after RNAi-knock-down of *Tc-foxQ2*, the CX is disturbed (Kitzmann et al., 2017). Therefore, we
268 hypothesized that the *Tc-foxQ2* might mark cells contributing to the CX. In order to test this we analyzed

269 larval (L5) and adult brains, where the CB is marked by a glia sheet (white arrowheads in Fig. 5C', F).
270 Indeed, EGFP marked projections contributed to the upper division (fan shaped body) of the CB (white
271 arrowheads in Fig. 5C, E) while another fascicle crossed the midline directly dorsal of the CB (dorsal with
272 respect to neuraxis; open arrowhead in Fig. 5E').

273 In summary, we found that *Tc-foxQ2* positive cells formed three cell clusters in the protocerebrum that
274 projected through the early brain commissure. Later, they marked specific subsets of midline fascicles of
275 the developing central brain and eventually contributed to the upper unit of the central body and to
276 subsets of brain commissures.

277 Some additional *Tc-foxQ2*⁺ cells merit mentioning although they were not neural or did not contribute to
278 the central brain. Firstly, cells of the stomodeum except for the dorsal roof were marked at all stages
279 (Fig. 3 and white arrowheads in Fig. S5). The domain appeared to be continuous with an expression in
280 the lateral parts of the labrum from stage NS14 onwards (open arrowheads in Fig. S5). Secondly, several
281 *Tc-foxQ2*⁺ cells lateral to the stomodeum were observed at NS13 (open arrowhead in Fig. S6A). From NS
282 14 onwards they had expanded to a group of cells adjacent to the stomodeum, which sent projections
283 into the posterior circumesophageal commissure (open arrowhead in Fig. S6B). Thirdly, about 12 weakly
284 stained cells were closely attached to the developing commissure at the midline (n=5; star in Fig. 4A';
285 Table S5). These cells were Tc-FoxQ2 protein negative at NS13 but could have retained EGFP signal from
286 median cells marked at a previous stage (e.g. dorsal to the stomodeum at NS6; see Fig. 3B').

287

288 [In vivo imaging reveals complex morphogenetic movements of the developing brain](#)

289 In order to confirm our view on the morphogenetic behavior of the marked cell clusters we used light-
290 sheet based fluorescence microscopy for in vivo imaging (Strobl et al., 2015). We imaged a cross of the
291 *foxQ2-5'-line* with the *AGOC #6* reporter, which marks glia cells via the 3XP3 promoter (Koniszewski et
292 al., 2016; Strobl et al., 2018). Three prominent morphogenetic movements were revealed: Initially, both
293 brain and stomodeum EGFP signals started out in close vicinity at the dorsal side (Fig. 6A white
294 arrowhead and white arrow, respectively). Shortly later, the stomodeum became elongated and bent
295 away towards the ventral side such that the initially adjacent expression domains came to lie on opposite
296 sides of the brain (Fig. 6B-C). At the same time a second movement was observed, where the bilateral
297 *Tc-foxQ2*⁺ cell clusters converged from lateral positions towards the midline until they made contact at
298 the medial brain (white arrowheads in Fig. 6E-J). The third movement consisted of an overall ventral
299 bending of the head and brain where the relative positions of the expression domains remained similar
300 (compare white lines in Fig. 6C and D). These movements reflected the movements described by the
301 "bend and zipper" model of head development (Posnien and Bucher, 2010; Posnien et al., 2010). Both
302 the *anterior-median-foxQ2-cluster* (white arrowheads in Fig. 6E-J) and the *lateral-foxQ2-lineage* (orange
303 arrowheads) could be followed throughout development confirming our results in fixed specimen.

304

305 [Arrest of central brain formation in *Tc-foxQ2* RNAi embryos](#)

306 Development of the commissures is quite different in the protocerebrum compared to segmental
307 ganglia. The initially compact primary brain commissure later expands into a broad field containing
308 several midline crossing fascicles. Another difference is the subsequent formation of the CB by de- and
309 re-fasciculation of axon tracts from a subset of these commissures (Boyan et al., 2017). Given the
310 contribution of *Tc-foxQ2*⁺ cells to the primary commissure and other midline spanning structures, we

311 asked whether it was required for splitting of the primary brain commissures. In order to test this, we
312 knocked down *Tc-foxQ2* function by RNAi and stained the knock-down embryos with acetylated tubulin
313 (acTub). We found that the primary brain commissure formed but was slightly irregular at NS13
314 (compare white arrowheads in Fig. 7A and B). This was in line with our finding that *Tc-foxQ2* positive
315 neurons do not pioneer the commissure but project into it shortly after its formation. Some anterior
316 aberrations stemmed from the previously described loss of the labrum (white arrows in Fig. 7A, B)
317 (Kitzmann et al., 2017). In wildtype NS15 embryos, the brain primordium had increased in size by
318 additional fascicles, the primary commissure had split and first chiasmata had formed (white arrowhead
319 in Fig. 7C). Strikingly, this process was not observed in *Tc-foxQ2* RNAi animals with strong phenotype.
320 Here, the primary commissure remained compact without signs of splitting (white arrowhead in Fig. 7D).
321 As a consequence, the brain neuropil remained extremely narrow (compare the space between the cell
322 bodies in Fig. 7C' and D', open arrowheads). Lateral to the central body, the basic architecture of
323 fascicles emanating from the commissure was mostly intact (e.g. the formation of three main branches
324 emanating from the central brain (arrows in Fig. 7D)) although it appeared to be built by fewer neurons.
325 As a consequence, the lateral neuropil area was reduced as well (open arrowheads in Fig. 7D', E'). In
326 weak phenotypes, commissure splitting had occurred to some degree but the arrangement of fascicles
327 was clearly abnormal (white arrowhead in Fig. 7E). In summary, *Tc-foxQ2* function is essential for
328 splitting of the brain commissure and for the expansion of the protocerebral neuropil, which together
329 constitute the central brain anlagen. As a consequence, CB development was abolished. Hence, crucial
330 steps of protocerebrum specific features depend on *Tc-foxQ2* function.

331

332 Analyses in novel brain imaging lines reveals a role for *Tc-foxQ2* for different lineages

333 We wondered, in how far different neural lineages would be affected by *Tc-foxQ2* knock-down. To
334 that end, we established two novel transgenic imaging lines that mark subsets of neurons. E035004
335 is an enhancer trap line generated in the GEKU screen (Trauner et al., 2009). We found that the
336 insertion was in the *Tribolium Tenascin-a* locus and EGFP signal overlapped with anti-Ten-a antibody
337 staining (not shown). We call this line *Ten-a-green*. Like in *Drosophila*, *Ten-a-green* marked subsets
338 of axons of the embryonic CNS (Fascetti and Baumgartner, 2002). At NS15, three groups of cells
339 were marked. The anterior group contained approximately 39 cells (n=4; white circle in Fig. 8A;
340 Table S7) the posterior-lateral group around 32 cells (n=4; open arrowhead in Fig. 8A; Table S7) and
341 the posterior-median group comprised about 27 cells (n=4; dashed circle in Fig. 8A; Table S7). The
342 central brain primordium was marked with two *Ten-a* positive fascicles projecting across the midline
343 (white arrow in Fig. 8A marks one of them). These fascicles represented a subset of the acTub
344 positive commissures (compare to Fig. 8A'). Among other patterns circumesophageal projections
345 were found.

346

347 In *Tc-foxQ2* RNAi, the *Ten-a* positive commissure was highly reduced while the circumesophageal
348 projection was still found. The cell clusters were still discernable but the number of the cells was
349 reduced by half (Fig. 8B; Table S7).

350

351 Next we generated an enhancer construct by fusing the upstream regulatory region of *Tc-rx* to
352 *dsRedexpress* (*rx-5'-up* line; see Supplementary Materials and Methods for details). This line marked
353 an anterior median group of cells, which projected into the central brain (white circle and
354 arrowhead in Fig. 8C). In addition, a number of peripheral cells without projections into the central
355 brain was marked (open arrowhead in Fig. 8C). A subset of the marked cells was Tc-Rx positive but a

356 significant number was not (see Supplementary Materials and Methods and Fig. S7). Knock-down of
357 *Tc-foxQ2* led to a strong decrease of median cell number at NS15 to about 25% of wildtype (n=6;
358 Table S8) and to the complete loss of the marked brain commissures (white circle and arrowhead in
359 Fig. 8D). The number of peripheral marked cells was reduced as well. In summary, *Tc-foxQ2* knock-
360 down in our imaging lines confirmed the phenotype found in our acTub staining and showed that
361 different neural lineages were affected.

362

363 *Tc-foxQ2* function is required for survival of neural cells

364 Finally, we asked in how far EGFP expression of the *foxQ2-5'-line* would be affected by knocking down
365 *Tc-foxQ2*. Indeed, at NS13 we found strongly reduced number of cells (less than half; n=4; Table S9) in
366 the *anterior-median-foxQ2-cluster* (white arrowheads in Fig. 9A, B) while the *lateral-foxQ2-lineage* was
367 either absent or fused to the other cluster. The cells close to the stomodeum were lost completely (not
368 shown). The stomodeal expression, in contrast, appeared unaffected (stars in Fig. 9A, B). At NS15 the
369 number of neural cells remained less than half of wildtype (n=4; Table S9) but the remaining cells always
370 formed connections across the midline. However, these fascicles were thinner and followed an abnormal
371 rounded path instead of the straight line found in wildtype (compare white arrows in Fig. 9E and F).
372 These data indicated that *Tc-foxQ2* was required for survival of neural cells and that upon RNAi these
373 cells were lost by apoptosis. Indeed, increased cell death had been observed after *Tc-foxQ2* RNAi at NS13
374 (Kitzmann et al., 2017). The reduced number of *Tc-foxQ2*⁺ cells was likely the reason for the thinner
375 commissure while its altered path might be a secondary effect due to general misspecification in the
376 central brain after *Tc-foxQ2* RNAi (see below). The reduction of cell number could be due to apoptosis
377 after misspecification of cells due to lack of *Tc-foxQ2*. Alternatively, *Tc-foxQ2* could be involved in an
378 autoregulatory loop, which would lead to EGFP reduction in an RNAi background.

379

380

381

382

383

384

385

386

387

388 Discussion

389 Does *Tc-foxQ2* mark neuroblasts of both type I and II?

390 We propose that *Tc-foxQ2* is expressed in both type I and type II neuroblasts. Type I NBs divide
391 asymmetrically to form ganglion mother cells, which divide once more to form two postmitotic
392 neural cells (Technau et al., 2006). All neuroblasts of the ventral nerve cord and most
393 neuroblasts of the brain belong to the type I. Type II neuroblasts, in contrast, give rise to
394 intermediate neural progenitors (INPs), which themselves divide in a stem cell-like fashion to
395 form ganglion mother cells (GMCs) (Boone and Doe, 2008; Bowman et al., 2008; Boyan et al.,
396 2010). This division mode leads to an increased number of cells stemming from one neuroblast.
397 Interestingly, most of the columnar neurons of the central complex derive from type II neural
398 lineages (Boyan et al., 2010; Peraanu et al., 2011; Walsh and Doe, 2017). Unfortunately,
399 molecular markers for reliably distinguishing type I from type II neuroblasts remain to be
400 established in insects outside *Drosophila*. Nevertheless, we suggest that *Tc-foxQ2* marks both
401 types of neuroblasts. The *lateral-foxQ2-lineage* might be a type I lineage. First, it is located in a
402 lateral region in the neuroectoderm while type II neuroblasts were found in the anterior median
403 brain (Boyan and Williams, 2011; Walsh and Doe, 2017). Second, within this cluster we see only
404 one *Tc-ase* marked cell with neuroblast typical morphology throughout several stages of
405 development and the cluster eventually comprises a moderate number of neurons (15-20),
406 which is in the range typical of type I NBs. Finally, this group of cells is surrounded by one glial
407 sheet, which is indicative for neural lineages (Younossi-Hartenstein et al., 1996). The *anterior-*
408 *median-foxQ2-cluster*, by contrast, is likely built by one or more type II neuroblasts. First, the
409 number of *Tc-ase* positive cells in that region decreased over time. This would be rather unusual
410 for neuroblasts but would be expected for INPs and GMCs of a type II lineage, which express
411 *asense* as well (Álvarez and Díaz-Benjumea, 2018; Walsh and Doe, 2017). Further, the number of
412 *Tc-foxQ2* positive neurons within the single glia niche was much larger (>200 cells), which would
413 be in line with type II mode of division. Moreover, the projection patterns into the CX are
414 reminiscent of the one found in embryonic type II neuroblast lineages in *Drosophila* (Álvarez and
415 Díaz-Benjumea, 2018). However, we were not able to unequivocally show a contribution of *Tc-*
416 *foxQ2* positive cells to the WXYZ tracts, which was described for DM1-4 type II lineages in
417 *Drosophila* and *Schistocerca* (Boyan and Reichert, 2011). Hence, this hypothesis needs to be
418 further tested once reliable markers for type II neuroblasts are developed. It would be intriguing
419 to find one regulatory gene contributing to the specification of different types of neuroblasts,
420 which both contribute to the central complex.

421

422 How does *Tc-foxQ2* function in CX development?

423 *Tc-foxQ2* positive cells are contributing to the CX and *Tc-foxQ2* is essential for its development.
424 The contribution could affect several stages of CX development. First, the effect could be a
425 consequence of the failure of commissural splitting. In normal development, the primary brain
426 commissure splits into several fascicles, which is the prerequisite for subsequent central body
427 formation. Some neurites undergo fascicle switching, i.e. they leave their commissure (de-
428 fasciculation) and bridge to another commissure, which they join (re-fasciculation). As

429 consequence, these neurites form X-shaped crossings prefiguring the columns of the central
430 body (Boyan and Williams, 2011; Boyan et al., 2008; Boyan et al., 2017). In the absence of
431 commissural splitting, this process and central body formation cannot take place. A putative
432 second contribution of *Tc-foxQ2* could be to specify the points of fascicle switching. In the late
433 embryonic brain, *Tc-foxQ2* marks commissures that are located in the region where this process
434 will occur. In this model, *Tc-foxQ2* positive neurites could either be the ones that de-fasciculate
435 or they could be required to provide the signal for other neurites to do so. Indeed, we find *Tc-*
436 *foxQ2* positive fascicles closely associated with the larval central body. Due to the arrest of
437 development after the first phenotype, the other mechanism cannot be observed directly and
438 remains to be tested. Scrutinizing the development of individual *Tc-foxQ2* positive cells would
439 be helpful. Actually, we have designed our enhancer trap line to express Cre along with EGFP.
440 Therefore, once a transgenic *Tribolium* line with a functional brainbow construct is developed,
441 single neurons within the *Tc-foxQ2* positive clusters can be traced (Livet et al., 2007).

442

443 [Making the protocerebrum different from segmental ganglia](#)

444 Our results show that *Tc-foxQ2* is one of the regulatory genes required for the development of
445 structures that distinguish the protocerebrum from segmental ganglia. Specifically, it is involved
446 in the unique development of the brain commissures and the midline spanning neuropils of the
447 central complex. We found several protocerebrum-specific functions. First, *Tc-foxQ2* is
448 expressed in neural progenitors of the protocerebrum but not in the more posterior ganglia.
449 Hence, *Tc-foxQ2* has indeed the potential of contributing to developmental programs that are
450 specific to this brain part. Therefore, this gene adds to the list of co-expressed genes assumed to
451 specify NB identity in the *Drosophila* brain (Urbach and Technau, 2003a). A second
452 protocerebrum-specific role is the contribution of *Tc-foxQ2* positive neurons to the CX. Third,
453 *Tc-foxQ2* positive neurons mark subsets of axons within the early brain commissure ending up
454 in different commissural fascicles after the split of the primary commissure. This commissural
455 splitting is observed only in the protocerebrum (Boyan et al., 2008; Boyan et al., 2017). The third
456 and most striking role of *Tc-foxQ2* in making the protocerebrum different from the segmental
457 ganglia is the requirement for commissure splitting. As consequence, the protocerebrum-
458 specific formation of an extended central brain neuropil with several commissures is blocked
459 giving the commissure a more segmental like appearance.

460 [Evolutionary relationship of apical organ and the central complex](#)

461 *foxQ2* together with *six3* and other genes are part of the anterior gene regulatory network
462 (aGRN) in animals and they contribute to the development of anterior-most neural structures.
463 Specifically, they are involved in patterning the apical organ/apical tuft including serotonergic
464 and neurosecretory cells in marine larvae, cnidarians, annelids and sea urchins (Leclère et al.,
465 2016; Marlow et al., 2014; Yaguchi et al., 2008). However, apical organs are usually lost during
466 metamorphosis and clear homologs were not found in neither insects nor vertebrates (Nielsen,
467 2005). Correlation of the aGRN with neuroendocrine cells was found in animals of all phyla
468 including arthropods (Hunnekuhl and Akam, 2014; Oliver et al., 1995; Posnien et al., 2011b;

469 Steinmetz et al., 2010). A potential role of *Tc-six3* and *Tc-foxQ2* in *Tribolium* brain development
470 had been noted but a detailed analysis of the respective brain phenotypes had not been
471 performed and the projection patterns of these cells had not been studied in any insect
472 (Kitzmann et al., 2017; Posnien et al., 2011b).

473 In this work we used *Tc-foxQ2* as a very specific marker for a subset of cells deriving from the
474 aGRN region (Kitzmann et al., 2017). Surprisingly, our data revealed for the first time a
475 contribution of these cells to the brain commissure and to the CX. A canonical CX is found in
476 crustaceans while homology of brain midline structures of other arthropods with the CX remain
477 equivocal (Hanström, 1928; Holmgren, 1916; Loesel et al., 2002; Loesel et al., 2011; Strausfeld,
478 2012). A contribution of the apical organ to brain development has been suggested in the
479 annelid *Platynereis dumerilii*, where the apical organ may provide an initial scaffold for the
480 developing anterior brain (Marlow et al., 2014). In the millipede *Strigamia maritima*, *foxQ2*
481 positive cells located at the brain midline build an early axonal scaffold forming a midline brain
482 structure from which longitudinal tracts project bilaterally into the trunk (Hunnekuhl and Akam,
483 2014). Based on these findings, we suggest a model, where ancestrally the apical organ
484 provided a scaffold for subsequent neural development of the anterior brain. In basal
485 arthropods like myriapods, the initially simple midline structure derived from the apical organ
486 expanded to form a prominent midline structure, which was still comparably simple. The
487 respective neurons provided a more prominent scaffold for subsequent neural development. In
488 crustaceans, this simple architecture was further developed to build a more elaborate CX, which
489 in stomatopods and insects reached its most complex realization (Thoen et al., 2017).

490 Outlook

491 *foxQ2* is one of several genes with an almost exclusive anterior expression in animals. We show
492 its crucial contribution to protocerebrum-specific development. Based on this, it seems
493 imperative that other highly conserved and protocerebrum-specific genes be considered when
494 investigating brain development (e.g. *rx*, *six3*, *chx*, *fez1*, etc.) (Kitzmann et al., 2017; Posnien et
495 al., 2011b). An approach focusing on genes known from the ventral nerve cord might fall short
496 of important insights. Given the rather exclusive contribution of *foxQ2* positive neurons, it will
497 be important to determine their individual projection patterns in both *Drosophila* and *Tribolium*
498 in order to map them with identified neurons from existing resources and to determine the
499 degree of conservation. Importantly, our concept of genetic neural lineages turned out to work
500 quite well and opens the way for such comparative studies (Koniszewski et al., 2016). Finally,
501 the evolution of *foxQ2* positive neurons provide an interesting study case for neural evolution:
502 From a role in patterning a rather simple structure, the apical organ, they expanded their role in
503 arthropods contributing to one of the most intricate insect brain structures. On the other hand,
504 *foxQ2* was lost in amphibians and mammals, which is astonishing regarding the usually high
505 degree of conservation of anterior regulators.

506

507 **Materials and methods**

508 **Animals**

509 Animals were reared under standard conditions at 32°C. The *San Bernadino (SB)* wild-type strain was used
510 for fluorescent in situ hybridization, antibody staining and RNAi experiments. The *Tc-vermillion^{white} (Tc-vw)*
511 strain (Lorenzen et al., 2002) was used for transgenesis.

512 **Generation of a Tc-FoxQ2 antibody**

513 The C-terminus (encoding for amino acids 202–286) was amplified from cDNA and cloned into pET SUMO
514 vector, generating a fusion protein with a His-SUMO tag and expressed in BL21-DE3 Rosetta cells. Protein
515 purification was done with Ni²⁺ chelate affinity chromatography. The antibody was produced in guinea pigs
516 by Eurogentec (Liège, Belgium).

517 **Generation of imaging lines and stocks**

518 *foxQ2-5'-line*: two guide RNAs (gRNAs) targeting the upstream region of *Tc-foxQ2* were designed with
519 the aid of the flyCRISPR Optimal Target Finder (<http://tools.flycrispr.molbio.wisc.edu/targetFinder/>)
520 (Gratz et al., 2014). The gRNA was cloned into the vector p(TcU6b-*Bsal*) following the protocol described
521 previously (Gilles et al., 2015). The repair template for NHEJ-mediated knock-in [3xP3:Tc'v-SV40-Cre-2A-
522 EGFP:bhsp68-eb] was cloned into the pJET1.2 vector (Addgene plasmid #124068). For linearizing the
523 plasmid, an *Dm-ebony* target site (gRNA-eb) was added. The helper plasmid p(bhsp68-Cas9) expressing
524 Cas9 was a gift from Michalis Averof (Addgene plasmid #65959). Embryonic injections were performed
525 as previously described (Berghammer et al., 2009). The final concentrations of the helper plasmid and
526 the repair plasmid was 500 ng/μl each, and 125 ng/μl for each gRNA. A protocol is published in
527 (Farnworth et al., in press). *rx-line*: The construct [rx-5'up:DsRedEx-SV40] contains 6 kb of upstream
528 regulatory region and the endogenous promoter of the *Tc-rx* gene and the reporter gene DsRedExpress.
529 piggyback mediated transgenesis was performed in the Tc-vw strain.

530

531 **RNAi**

532 Both dsRNA fragment and parental injection was performed as in (Kitzmann et al., 2017), where off target
533 controls had been performed. The injected dsRNA concentrations were 1.5 μg/μl and 3.0 μg/μl.

534 **Immunohistochemistry and FISH**

535 Immunostaining of embryonic, larval and adult brains were performed according to the described protocol
536 (Büscher et al., in press; Hunnekuhl et al., in press). FISH was performed using a horseradish peroxidase
537 (POD) mediated tyramide signal amplification (TSA). Primary antibodies: chicken anti-GFP (1:1000,
538 Abcam), mouse anti-ac.Tubulin (1:50, Sigma), mouse anti-Synapsin (1:40, DHSB Hybridoma Bank), rabbit
539 anti-DsRed (1:1000, Abcam). Secondary antibodies coupled with Alexa Fluor 488 or Alexa Fluor 555
540 (Thermo Fisher Scientific) were used at 1:1000.

541 **In vivo imaging**

542 Long-term live imaging was performed with digitally scanned laser light sheet-based fluorescence
543 microscopy (DSLIM, LSFM) as described previously for *Tribolium* (Strobl et al., 2015; Strobl et al., 2017)(
544 In brief, embryos were collected either (i) from a homozygous *foxQ2-5'* culture or (ii) from two hybrid
545 cultures that consisted either of homozygous *foxQ2-5'* females mated with (mO-mC/mO-mC)
546 homozygous AGOC #6 males or of (mO-mC/mO-mC) homozygous AGOC #6 females mated with
547 homozygous *foxQ2-5'* females. After one hour of collection at 25°C, embryos were incubated for 20
548 hours at 32°C. Sample preparation took approximately one hour at room temperature (23±1°C), so that
549 embryos were at the beginning of germband retraction. Embryos were recorded either (i) only along the
550 dorsal axis or (ii) along the dorsal and lateral axis with an interval of 60 minutes. All shown embryos
551 survived the imaging procedure, developed to healthy and fertile adults, and when mated either (i) with
552 a homozygous *foxQ2-5'* sibling or (ii) with a (mO-mC/mO-mC) homozygous AGOC #6 sibling, produced
553 progeny that was also fertile. Metadata of the three datasets is provided with the Zenodo dataset.

554 **Image processing and documentation**

555 Immunohistochemistry and FISH were imaged using a ZEISS laser scanning microscope LSM510. Stacks
556 were processed using ImageJ (v.1.47). Images were level-adjusted for brightness and contrast and
557 assembled in Photoshop CS (Adobe). The stacks are available in both original Zeiss LSM format and as avi
558 on figshare (<https://figshare.com/account/home#/projects/62939>).

559

560

561 **Acknowledgements**

562 We thank Natalia Carolina García Pérez and Rebekka Wallrafen for mapping and initial characterization
563 of the *Ten-a line* and Achim Dickmanns' (GZMB) help with the purification of the protein. Kolja
564 Eckermann for providing the SUMO plasmid and Vera Hunnekuhl for valuable comments on the
565 manuscript. In vivo imaging was performed with the infrastructure provided by Ernst Stelzer. Elke Küster
566 helped identifying and keeping the transgenic stocks.

567

568 **Competing interests**

569 The authors declare no competing interests.

570 **Funding**

571 This work was supported by a fellowship from the Chinese Scholarship Council (CSC) to B.H.
572 [201406350036 and a Heisenberg professorship from Deutsche Forschungsgemeinschaft to G.B.
573 [DFG BU1443/10].

574 **Data availability**

575 All LSM stacks can be downloaded from the figshare repository
576 (<https://figshare.com/account/home#/projects/62939>). The construct used for generating the
577 enhancer trap is available from AddGene (#124068). The in vivo imaging data is accessible at
578 Zenodo (10.5281/zenodo.2645645 Dataset DS0001 / "left part" of Figure 6 and Supplementary

579 Movie X; 10.5281/zenodo.2645657 Dataset DS0002; 10.5281/zenodo.2645665 Dataset DS0003
580 / "right part" of Figure 6 and Supplementary Movie X+1)

581

582 **References**

- 583 **Acampora, D., Avantaggiato, V., Tuorto, F., Barone, P., Reichert, H., Finkelstein, R. and Simeone, A.**
584 (1998). Murine Otx1 and Drosophila otd genes share conserved genetic functions required in
585 invertebrate and vertebrate brain development. *Development* **125**, 1691–702.
- 586 **Álvarez, J.-A. and Díaz-Benjumea, F. J.** (2018). Origin and specification of type II neuroblasts in the
587 Drosophila embryo. *Dev. Camb. Engl.* **145**,.
- 588 **Arendt, D. and Nübler-Jung, K.** (1996). Common ground plans in early brain development in mice and
589 flies. *Bioessays* **18**, 255–9.
- 590 **Arendt, D., Denes, A. S., Jekely, G. and Tessmar-Raible, K.** (2008). The evolution of nervous system
591 centralization. *Philos Trans R Soc Lond B Biol Sci* **363**, 1523–8.
- 592 **Berghammer, A. J., Klingler, M. and Wimmer, E. A.** (1999). A universal marker for transgenic insects.
593 *Nature* **402**, 370–1.
- 594 **Berghammer, A. J., Weber, M., Trauner, J. and Klingler, M.** (2009). Red flour beetle (*Tribolium*) germline
595 transformation and insertional mutagenesis. *Cold Spring Harb. Protoc.* **2009**, pdb.prot5259.
- 596 **Biffar, L. and Stollewerk, A.** (2014). Conservation and evolutionary modifications of neuroblast
597 expression patterns in insects. *Dev. Biol.* **388**, 103–116.
- 598 **Boone, J. Q. and Doe, C. Q.** (2008). Identification of Drosophila type II neuroblast lineages containing
599 transit amplifying ganglion mother cells. *Dev. Neurobiol.* **68**, 1185–1195.
- 600 **Bowman, S. K., Rolland, V., Betschinger, J., Kinsey, K. A., Emery, G. and Knoblich, J. A.** (2008). The
601 tumor suppressors Brat and Numb regulate transit-amplifying neuroblast lineages in Drosophila.
602 *Dev. Cell* **14**, 535–546.
- 603 **Boyan, G. S. and Reichert, H.** (2011). Mechanisms for complexity in the brain: generating the insect
604 central complex. *Trends Neurosci.* **34**, 247–257.
- 605 **Boyan, G. and Williams, L.** (2011). Embryonic development of the insect central complex: insights from
606 lineages in the grasshopper and Drosophila. *Arthropod Struct. Dev.* **40**, 334–348.
- 607 **Boyan, G. S., Williams, J. L. D. and Herbert, Z.** (2008). Fascicle switching generates a chiasmatal
608 neuroarchitecture in the embryonic central body of the grasshopper *Schistocerca gregaria*.
609 *Arthropod Struct. Dev.* **37**, 539–544.
- 610 **Boyan, G., Williams, L., Legl, A. and Herbert, Z.** (2010). Proliferative cell types in embryonic lineages of
611 the central complex of the grasshopper *Schistocerca gregaria*. *Cell Tissue Res.* **341**, 259–277.
- 612 **Boyan, G., Liu, Y., Khalsa, S. K. and Hartenstein, V.** (2017). A conserved plan for wiring up the fan-
613 shaped body in the grasshopper and Drosophila. *Dev. Genes Evol.* **227**, 253–269.
- 614 **Bucher, G., Scholten, J. and Klingler, M.** (2002). Parental RNAi in *Tribolium* (Coleoptera). *Curr. Biol.* **12**,
615 R85–R86.

- 616 **Büscher, M., Oberhofer, G., García-Pérez, N. C. and Bucher, G.** (in press). A protocol for double
617 fluorescent in situ hybridization and immunohistochemistry for the study of embryonic brain
618 development in *Tribolium castaneum*. In *Methods in Brain Development*, p. Springer Nature.
- 619 **Darras, S., Gerhart, J., Terasaki, M., Kirschner, M. and Lowe, C. J.** (2011). -Catenin specifies the
620 endomesoderm and defines the posterior organizer of the hemichordate *Saccoglossus*
621 *kowalevskii*. *Development* **138**, 959–970.
- 622 **Dönitz, J., Gerischer, L., Hahnke, S., Pfeiffer, S. and Bucher, G.** (2018). Expanded and updated data and a
623 query pipeline for iBeetle-Base. *Nucleic Acids Res.* **46**, D831–D835.
- 624 **Dunn, E. F., Moy, V. N., Angerer, L. M., Angerer, R. C., Morris, R. L. and Peterson, K. J.** (2007). Molecular
625 paleoecology: using gene regulatory analysis to address the origins of complex life cycles in the
626 late Precambrian. *Evol. Dev.* **9**, 10–24.
- 627 **El Jundi, B. and Heinze, S.** (2016). *Three-dimensional atlases of insect brains*. New York: Springer
628 (Humana Press).
- 629 **Farnworth, S. M., Eckermann, K. N., Ahmed, H. M. M., Mühlen, D. S., He, B. and Bucher, G.** (in press).
630 The red flour beetle as model for comparative neural development: Genome editing to mark
631 neural cells in *Tribolium* brain development. In *Methods in Brain Development*, .
- 632 **Fascetti, N. and Baumgartner, S.** (2002). Expression of *Drosophila* Ten-a, a dimeric receptor during
633 embryonic development. *Mech. Dev.* **114**, 197–200.
- 634 **Fritzenwanker, J. H., Gerhart, J., Freeman, R. M. and Lowe, C. J.** (2014). The Fox/Forkhead transcription
635 factor family of the hemichordate *Saccoglossus kowalevskii*. *EvoDevo* **5**, 17.
- 636 **Gehring, W. J.** (1996). The master control gene for morphogenesis and evolution of the eye. *Genes Cells*
637 **1**, 11–5.
- 638 **Gilles, A. F., Schinko, J. B. and Averof, M.** (2015). Efficient CRISPR-mediated gene targeting and
639 transgene replacement in the beetle *Tribolium castaneum*. *Dev. Camb. Engl.* **142**, 2832–2839.
- 640 **Gratz, S. J., Ukken, F. P., Rubinstein, C. D., Thiede, G., Donohue, L. K., Cummings, A. M. and O'Connor-**
641 **Giles, K. M.** (2014). Highly specific and efficient CRISPR/Cas9-catalyzed homology-directed repair
642 in *Drosophila*. *Genetics* **196**, 961–971.
- 643 **Hanström, B.** (1928). *Vergleichende Anatomie des Nervensystems der Wirbellosen Tiere unter*
644 *Berücksichtigung seiner Funktion*. Berlin: Springer-Verlag.
- 645 **Hartenstein, V. and Stollewerk, A.** (2015). The evolution of early neurogenesis. *Dev. Cell* **32**, 390–407.
- 646 **Hirth, F., Therianos, S., Loop, T., Gehring, W. J., Reichert, H. and Furukubo-Tokunaga, K.** (1995).
647 Developmental defects in brain segmentation caused by mutations of the homeobox genes
648 orthodenticle and empty spiracles in *Drosophila*. *Neuron* **15**, 769–78.
- 649 **Hirth, F., Kammermeier, L., Frei, E., Walldorf, U., Noll, M. and Reichert, H.** (2003). An urbilaterian origin
650 of the tripartite brain: developmental genetic insights from *Drosophila*. *Development* **130**, 2365–
651 73.

- 652 **Holmgren, N. F.** (1916). Zur vergleichenden Anatomie des Gehirns von Polychaeten, Onychophoren,
653 Xiphosuren, Arachniden, Crustaceen, Myriapoden, und Insekten. Vorstudien zu einer Phylogenie
654 der Arthropoden. *K. Sven. Vetenskapsakad Handl.* **56**, 1–303.
- 655 **Hunnekuhl, V. S. and Akam, M.** (2014). An anterior medial cell population with an apical-organ-like
656 transcriptional profile that pioneers the central nervous system in the centipede *Strigamia*
657 *maritima*. *Dev. Biol.* **396**, 136–149.
- 658 **Hunnekuhl, V. S., Farnworth, M. S. and Bucher, G.** (in press). Immunohistochemistry and fluorescent
659 whole mount RNA in situ hybridization in larval and adult brains of *Tribolium*. In *Methods in*
660 *Brain Development*, p. Springer Nature.
- 661 **Kittelmann, S., Ulrich, J., Posnien, N. and Bucher, G.** (2013). Changes in anterior head patterning
662 underlie the evolution of long germ embryogenesis. *Dev. Biol.* **374**, 174–184.
- 663 **Kitzmann, P., Weißkopf, M., Schacht, M. I. and Bucher, G.** (2017). A key role for foxQ2 in anterior head
664 and central brain patterning in insects. *Dev. Camb. Engl.* **144**, 2969–2981.
- 665 **Koniszewski, N. D. B., Kollmann, M., Bigam, M., Farnworth, M., He, B., Büscher, M., Hütteroth, W.,**
666 **Binzer, M., Schachtner, J. and Bucher, G.** (2016). The insect central complex as model for
667 heterochronic brain development-background, concepts, and tools. *Dev. Genes Evol.* **226**, 209–
668 219.
- 669 **Lai, S.-L. and Doe, C. Q.** (2014). Transient nuclear Prospero induces neural progenitor quiescence. *eLife*
670 **3**.
- 671 **Leclère, L., Bause, M., Sinigaglia, C., Steger, J. and Rentzsch, F.** (2016). Development of the aboral
672 domain in *Nematostella* requires β -catenin and the opposing activities of Six3/6 and Frizzled5/8.
673 *Dev. Camb. Engl.* **143**, 1766–1777.
- 674 **Lee, H.-H. and Frasch, M.** (2004). Survey of forkhead domain encoding genes in the *Drosophila* genome:
675 Classification and embryonic expression patterns. *Dev. Dyn.* **229**, 357–366.
- 676 **Livet, J., Weissman, T. A., Kang, H., Draft, R. W., Lu, J., Bennis, R. A., Sanes, J. R. and Lichtman, J. W.**
677 (2007). Transgenic strategies for combinatorial expression of fluorescent proteins in the nervous
678 system. *Nature* **450**, 56–62.
- 679 **Loesel, R., Nässel, D. R. and Strausfeld, N. J.** (2002). Common design in a unique midline neuropil in the
680 brains of arthropods. *Arthropod Struct. Dev.* **31**, 77–91.
- 681 **Loesel, R., Seyfarth, E.-A., Bräunig, P. and Agricola, H.-J.** (2011). Neuroarchitecture of the arcuate body
682 in the brain of the spider *Cupiennius salei* (Araneae, Chelicerata) revealed by allatostatin-,
683 proctolin-, and CCAP-immunocytochemistry and its evolutionary implications. *Arthropod Struct.*
684 *Dev.* **40**, 210–220.
- 685 **Lorenzen, M. D., Brown, S. J., Denell, R. E. and Beeman, R. W.** (2002). Cloning and characterization of
686 the *Tribolium castaneum* eye-color genes encoding tryptophan oxygenase and kynurenine 3-
687 monooxygenase. *Genetics* **160**, 225–234.

- 688 **Lowe, C. J., Wu, M., Salic, A., Evans, L., Lander, E., Stange-Thomann, N., Gruber, C. E., Gerhart, J. and**
689 **Kirschner, M.** (2003). Anteroposterior patterning in hemichordates and the origins of the
690 chordate nervous system. *Cell* **113**, 853–65.
- 691 **Marlow, H., Matus, D. Q. and Martindale, M. Q.** (2013). Ectopic activation of the canonical wnt signaling
692 pathway affects ectodermal patterning along the primary axis during larval development in the
693 anthozoan *Nematostella vectensis*. *Dev. Biol.* **380**, 324–334.
- 694 **Marlow, H., Tosches, M. A., Tomer, R., Steinmetz, P. R., Lauri, A., Larsson, T. and Arendt, D.** (2014).
695 Larval body patterning and apical organs are conserved in animal evolution. *BMC Biol.* **12**, 7.
- 696 **Mazet, F., Yu, J.-K., Liberles, D. A., Holland, L. Z. and Shimeld, S. M.** (2003). Phylogenetic relationships of
697 the Fox (Forkhead) gene family in the Bilateria. *Gene* **316**, 79–89.
- 698 **Nielsen, C.** (2005). Larval and adult brains. *Evol. Dev.* **7**, 483–489.
- 699 **Oliver, G., Mailhos, A., Wehr, R., Copeland, N. G., Jenkins, N. A. and Gruss, P.** (1995). Six3, a murine
700 homologue of the sine oculis gene, demarcates the most anterior border of the developing
701 neural plate and is expressed during eye development. *Development* **121**, 4045–55.
- 702 **Panov, A. A.** (1959). Structure of the insect brain at successive stages of postembryonic development. II.
703 the central body. *Entomol Rev* **38**, 276–283.
- 704 **Pereanu, W., Younossi-Hartenstein, A., Lovick, J., Spindler, S. and Hartenstein, V.** (2011). Lineage-based
705 analysis of the development of the central complex of the *Drosophila* brain. *J Comp Neurol* **519**,
706 661–89.
- 707 **Pfeiffer, K. and Homberg, U.** (2014). Organization and Functional Roles of the Central Complex in the
708 Insect Brain. *Annu. Rev. Entomol.* **59**, 165–184.
- 709 **Piperno, G. and Fuller, M. T.** (1985). Monoclonal antibodies specific for an acetylated form of alpha-
710 tubulin recognize the antigen in cilia and flagella from a variety of organisms. *J. Cell Biol.* **101**,
711 2085–2094.
- 712 **Posnien, N. and Bucher, G.** (2010). Formation of the insect head involves lateral contribution of the
713 intercalary segment, which depends on Tc-labial function. *Dev Biol* **338**, 107–16.
- 714 **Posnien, N., Schinko, J. B., Kittelmann, S. and Bucher, G.** (2010). Genetics, development and
715 composition of the insect head - A beetle's view. *Arthropod Struct Dev* **39**, 399–410.
- 716 **Posnien, N., Koniszewski, N. and Bucher, G.** (2011a). Insect Tc-six4 marks a unit with similarity to
717 vertebrate placodes. *Dev Biol* **350**, 208–216.
- 718 **Posnien, N., Koniszewski, N. D. B., Hein, H. J. and Bucher, G.** (2011b). Candidate Gene Screen in the Red
719 Flour Beetle *Tribolium* Reveals Six3 as Ancient Regulator of Anterior Median Head and Central
720 Complex Development. *PLoS Genet.* **7**, e1002418.
- 721 **Quiring, R., Walldorf, U., Kloter, U. and Gehring, W. J.** (1994). Homology of the eyeless gene of
722 *Drosophila* to the Small eye gene in mice and Aniridia in humans. *Science* **265**, 785–9.

- 723 **Range, R. C. and Wei, Z.** (2016). An anterior signaling center patterns and sizes the anterior
724 neuroectoderm of the sea urchin embryo. *Development*.
- 725 **Rempel, G. J.** (1975). The evolution of the insect head: the endless dispute. *Quaest. Entomol.* **11**, 7–25.
- 726 **Santagata, S., Resh, C., Hejzol, A., Martindale, M. Q. and Passamaneck, Y. J.** (2012). Development of
727 the larval anterior neurogenic domains of *Terebratalia transversa* (Brachiopoda) provides
728 insights into the diversification of larval apical organs and the spiralian nervous system. *EvoDevo*
729 **3**, 3.
- 730 **Schinko, J. B., Weber, M., Viktorinova, I., Kiupakis, A., Averof, M., Klingler, M., Wimmer, E. A. and**
731 **Bucher, G.** (2010). Functionality of the GAL4/UAS system in *Tribolium* requires the use of
732 endogenous core promoters. *BMC Dev Biol* **10**, 53.
- 733 **Schmitt-Engel, C., Schultheis, D., Schwirz, J., Ströhlein, N., Troelenberg, N., Majumdar, U., Dao, V. A.,**
734 **Grossmann, D., Richter, T., Tech, M., et al.** (2015). The iBeetle large-scale RNAi screen reveals
735 gene functions for insect development and physiology. *Nat. Commun.* **6**, 7822.
- 736 **Scholtz, G. and Edgecombe, G. D.** (2006). The evolution of arthropod heads: reconciling morphological,
737 developmental and palaeontological evidence. *Dev Genes Evol* **216**, 395–415.
- 738 **Sinigaglia, C., Busengdal, H., Leclère, L., Technau, U. and Rentzsch, F.** (2013). The Bilaterian Head
739 Patterning Gene *six3/6* Controls Aboral Domain Development in a Cnidarian. *PLoS Biol.* **11**,
740 e1001488.
- 741 **Skeath, J. B.** (1999). At the nexus between pattern formation and cell-type specification: the generation
742 of individual neuroblast fates in the *Drosophila* embryonic central nervous system. *Bioessays* **21**,
743 922–31.
- 744 **Snodgrass, R. E.** (1935). *Principles of Insect Morphology*. New York: McGraw Hill.
- 745 **Steinmetz, P. R., Urbach, R., Posnien, N., Eriksson, J., Kostyuchenko, R. P., Brena, C., Guy, K., Akam, M.,**
746 **Bucher, G. and Arendt, D.** (2010). *Six3* demarcates the anterior-most developing brain region in
747 bilaterian animals. *EvoDevo* **1**, 14.
- 748 **Strausfeld, N. J.** (2012). *Arthropod Brains - Evolution, Functional Elegance, and Historical Significance*.
749 New. Cambridge, Mass: Harvard University Press.
- 750 **Strobl, F., Schmitz, A. and Stelzer, E. H. K.** (2015). Live imaging of *Tribolium castaneum* embryonic
751 development using light-sheet-based fluorescence microscopy. *Nat. Protoc.* **10**, 1486–1507.
- 752 **Strobl, F., Klees, S. and Stelzer, E. H. K.** (2017). Light Sheet-based Fluorescence Microscopy of Living or
753 Fixed and Stained *Tribolium castaneum* Embryos. *J. Vis. Exp. JoVE*.
- 754 **Strobl, F., Anderl, A. and Stelzer, E. H.** (2018). A universal vector concept for a direct genotyping of
755 transgenic organisms and a systematic creation of homozygous lines. *eLife* **7**, e31677.
- 756 **Technau, G. M., Berger, C. and Urbach, R.** (2006). Generation of cell diversity and segmental pattern in
757 the embryonic central nervous system of *Drosophila*. *Dev Dyn* **235**, 861–9.

- 758 **Toen, H. H., Marshall, J., Wolff, G. H. and Strausfeld, N. J.** (2017). Insect-Like Organization of the
759 Stomatopod Central Complex: Functional and Phylogenetic Implications. *Front. Behav. Neurosci.*
760 **11**, 12.
- 761 **Tomoyasu, Y. and Denell, R. E.** (2004). Larval RNAi in *Tribolium* (Coleoptera) for analyzing adult
762 development. *Dev Genes Evol* **214**, 575–8.
- 763 **Trauner, J., Schinko, J., Lorenzen, M. D., Shippy, T. D., Wimmer, E. A., Beeman, R. W., Klingler, M.,**
764 **Bucher, G. and Brown, S. J.** (2009). Large-scale insertional mutagenesis of a coleopteran stored
765 grain pest, the red flour beetle *Tribolium castaneum*, identifies embryonic lethal mutations and
766 enhancer traps. *BMC Biol* **7**, 73.
- 767 **Urbach, R. and Technau, G. M.** (2003a). Molecular markers for identified neuroblasts in the developing
768 brain of *Drosophila*. *Development* **130**, 3621–37.
- 769 **Urbach, R. and Technau, G. M.** (2003b). Segment polarity and DV patterning gene expression reveals
770 segmental organization of the *Drosophila* brain. *Development* **130**, 3607–20.
- 771 **Urbach, R., Technau, G. M. and Breidbach, O.** (2003). Spatial and temporal pattern of neuroblasts,
772 proliferation, and Engrailed expression during early brain development in *Tenebrio molitor* L.
773 (Coleoptera). *Arthropod Struct. Dev.* **32**, 125–140.
- 774 **Walsh, K. T. and Doe, C. Q.** (2017). *Drosophila* embryonic type II neuroblasts: origin, temporal
775 patterning, and contribution to the adult central complex. *Dev. Camb. Engl.* **144**, 4552–4562.
- 776 **Weber, H.** (1966). *Grundriss der Insektenkunde*. 4th ed. Stuttgart: Gustav Fischer Verlag.
- 777 **Wegerhoff, R. and Breidbach, O.** (1992). Structure and development of the larval central complex in a
778 holometabolous insect, the beetle *Tenebrio molitor*. *Cell Tissue Res* **268**, 341–358.
- 779 **Wei, Z., Yaguchi, J., Yaguchi, S., Angerer, R. C. and Angerer, L. M.** (2009). The sea urchin animal pole
780 domain is a Six3-dependent neurogenic patterning center. *Development* **136**, 1179–89.
- 781 **Wheeler, S. R., Carrico, M. L., Wilson, B. A., Brown, S. J. and Skeath, J. B.** (2003). The expression and
782 function of the achaete-scute genes in *Tribolium castaneum* reveals conservation and variation
783 in neural pattern formation and cell fate specification. *Development* **130**, 4373–81.
- 784 **Yaguchi, S., Yaguchi, J., Angerer, R. C. and Angerer, L. M.** (2008). A Wnt-FoxQ2-Nodal Pathway Links
785 Primary and Secondary Axis Specification in Sea Urchin Embryos. *Dev. Cell* **14**, 97–107.
- 786 **Yaguchi, S., Yaguchi, J., Wei, Z., Shiba, K., Angerer, L. M. and Inaba, K.** (2010). ankAT-1 is a novel gene
787 mediating the apical tuft formation in the sea urchin embryo. *Dev. Biol.* **348**, 67–75.
- 788 **Younossi-Hartenstein, A., Nassif, C., Green, P. and Hartenstein, V.** (1996). Early neurogenesis of the
789 *Drosophila* brain. *J. Comp. Neurol.* **370**, 313–329.
- 790 **Yu, J.-K., Holland, N. D. and Holland, L. Z.** (2003). AmphiFoxQ2, a novel winged helix/forkhead gene,
791 exclusively marks the anterior end of the amphioxus embryo. *Dev. Genes Evol.* **213**, 102–105.

793 Figure legends

794

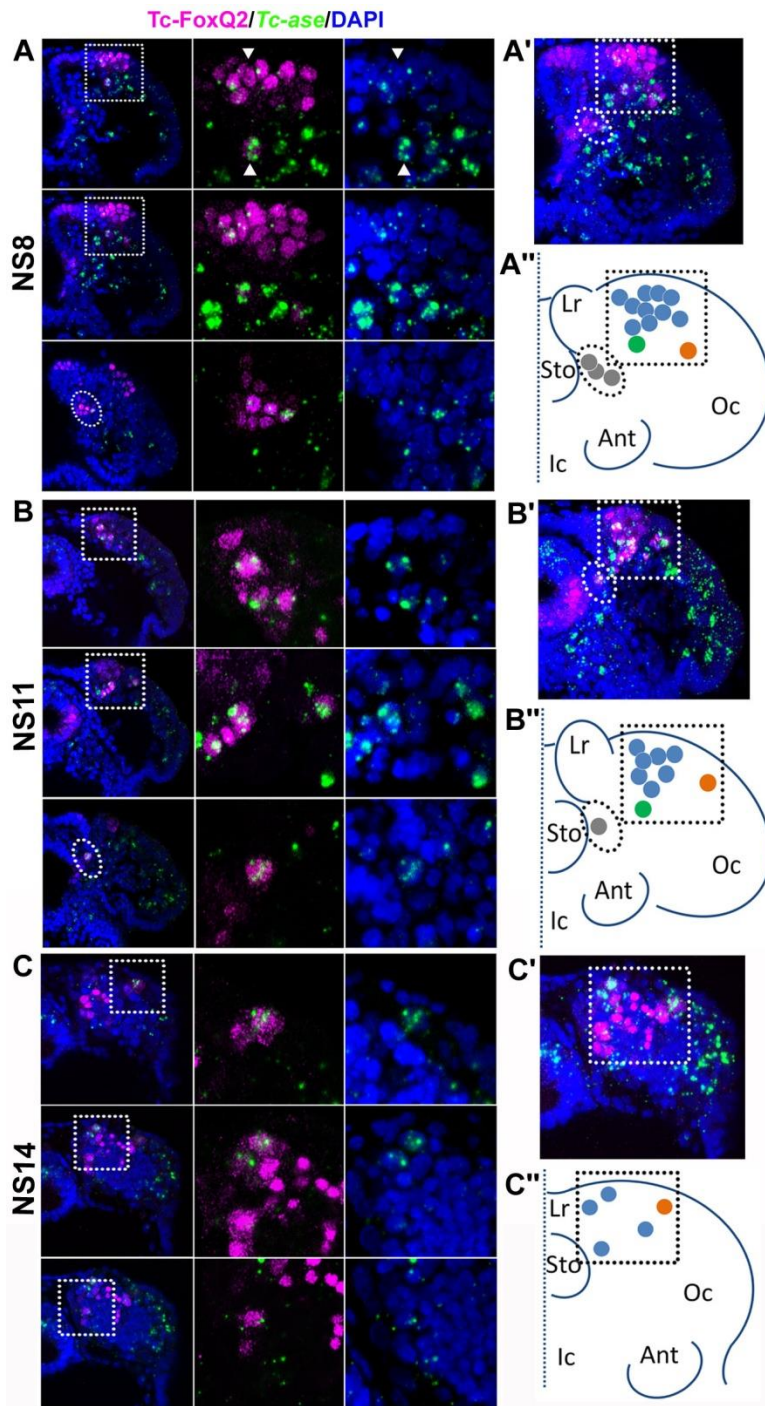


Fig. 1. Tc-FoxQ2 positive neural progenitor cells. Tc-FoxQ2 protein is visualized by immunohistochemistry at different stages (magenta) while neural progenitor cells (NPCs) are marked by intronic *Tc-ase* whole mount in situ hybridization (green). Nuclei are visualized by DAPI (blue). Optical sections of right halves of stained heads are shown in the left column while respective close-ups are shown in second and third column (see hatched areas in left column in A, B and C). A projection of all optical sections (A', B' and C') and a scheme (A'', B'' and C'') are given in the right column. (A-A'') At NS8 about 15 Tc-FoxQ2 positive NPCs are found (n=6). By position, three groups are distinguished: A large anterior median group (blue in A'') with one neuroblast slightly separated posteriorly (green in A''), one single lateral NPC (orange in A'') and a group located closely to the midline (grey in A''). White arrowheads show two exemplary NPCs. (B-B'') At NS11 about 10 Tc-FoxQ2 positive NPCs are observed (n=6). (C-C'') At NS14, the number has decreased to 5-7 cells (n=6). The single lateral NPC remains distinguishable (orange in C''). Lr: labrum; Sto: stomodeum; Oc: ocular region; Ant: antenna; Ic: Intercalary region.

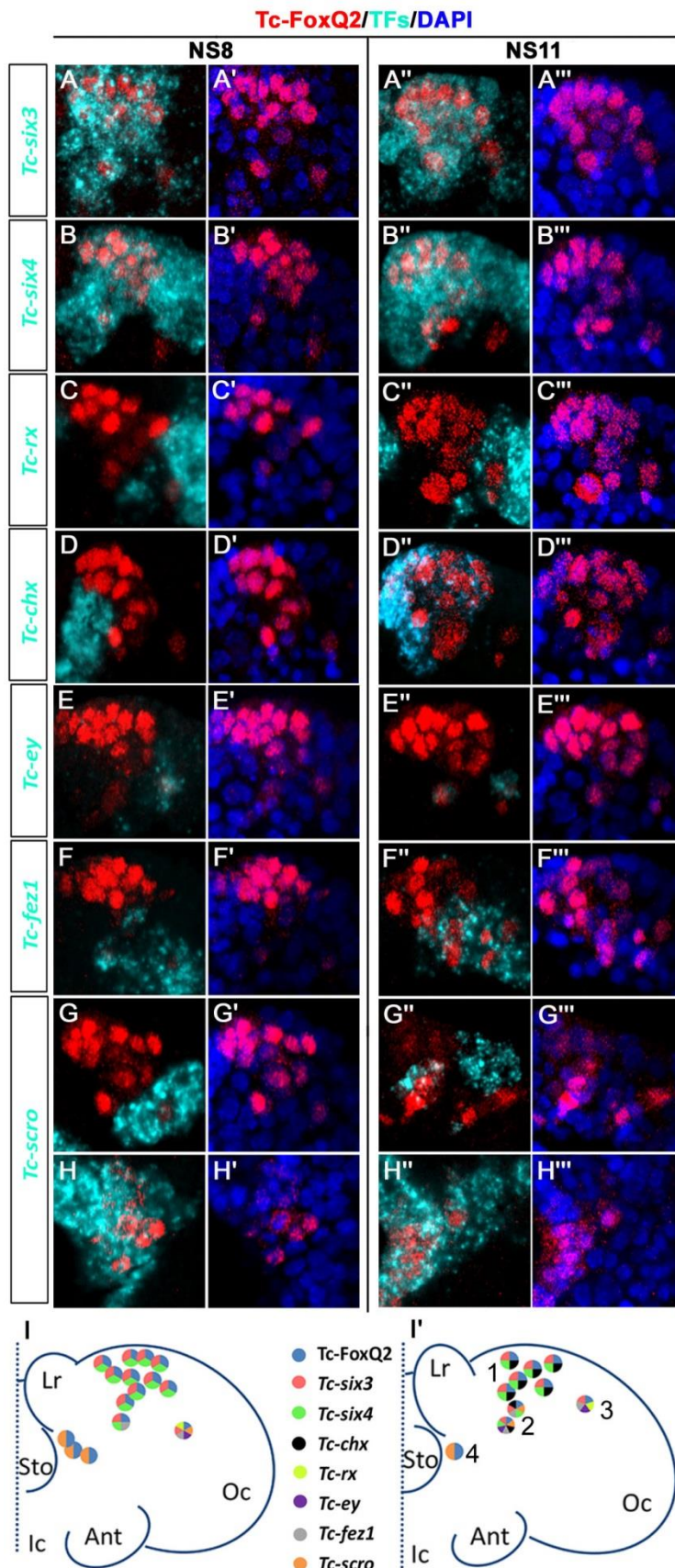
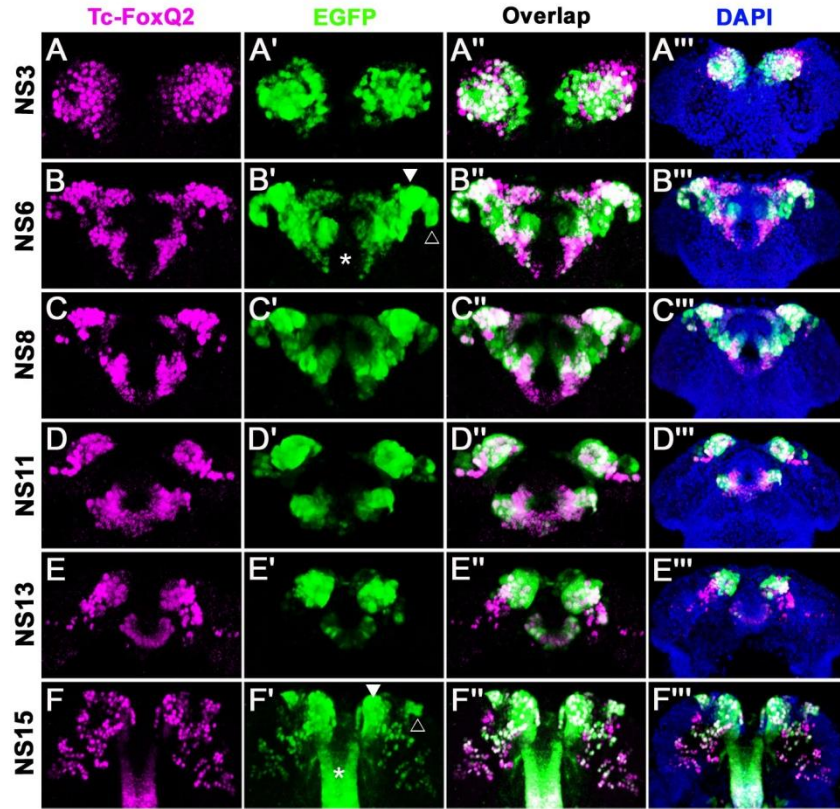


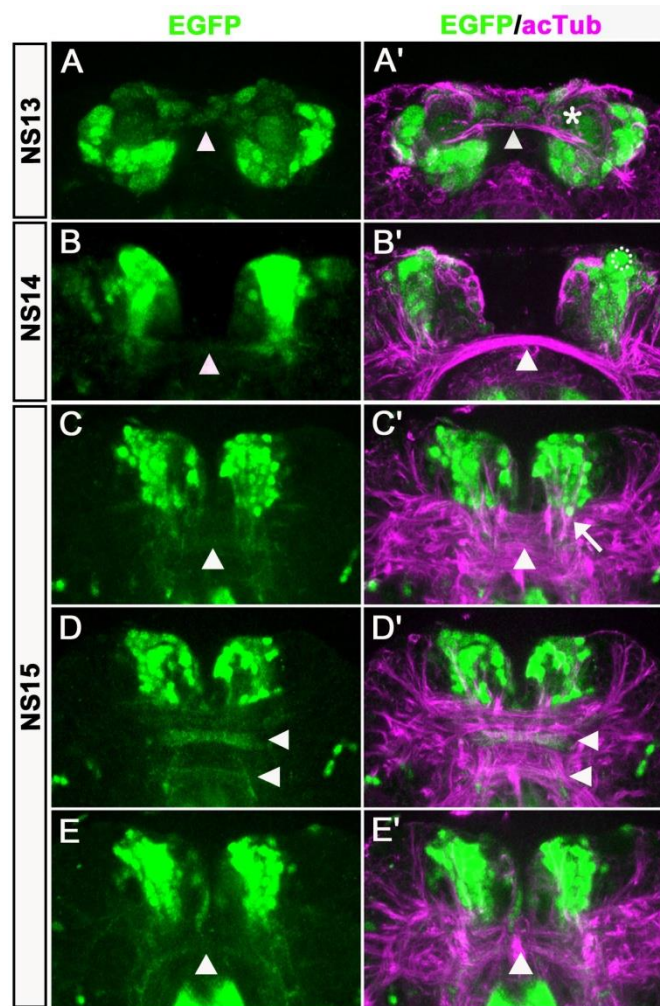
Fig. 2. Neural progenitor cells co-express transcription factors. Tc-FoxQ2 is visualized by immunohistochemistry (red) while the other transcription factors (TFs) are marked by *fluorescent in situ hybridization* (cyan) at NS8 and NS11. Nuclei are visualized by DAPI (blue). Close-ups of the right halves of embryonic heads are shown (A-H''') and schemes are given at the bottom (I and I'). (A-A''') Co-expression of *Tc-six3* and Tc-FoxQ2. (B-B''') Co-expression of *Tc-six4* and Tc-FoxQ2. (C-C''') Co-expression of *Tc-rx* and Tc-FoxQ2. (D-D''') Co-expression of *Tc-chx* and Tc-FoxQ2. (E-E''') Co-expression of *Tc-ey* and Tc-FoxQ2. (F-F''') Co-expression of *Tc-fez1* and Tc-FoxQ2. (G-H''') Co-expression of *Tc-scro* and Tc-FoxQ2. (I, I') Four different identities of NPCs are distinguished based on their position and co-expression. *P-fox-am* (1) is located in the anterior median neuroectoderm. The cells in this group co-express Tc-FoxQ2 with *Tc-six3*, *Tc-six4* and later *Tc-chx*. *P-fox-amp* (2) is located posteriorly adjacent with additional expression of *Tc-scro*, *Tc-fez1* and in one of the cells also *Tc-ey*. *P-fox-l* (3) consists of one lateral cell which co-expresses Tc-FoxQ2 with *Tc-six3*, *Tc-fez1*, *Tc-rx* and *Tc-ey*. *P-fox-v* (4) is located ventrally adjacent to the stomodaeum, showing only co-expression of Tc-FoxQ2 and *Tc-scro*. Same abbreviations as in Fig. 1.



863

864 **Fig. 3. *Tc-foxQ2* positive cells marked by antibody and the *foxQ2-5'-line*.** The expression of EGFP (green)
865 derived from the *foxQ2-5'-line* and Tc-FoxQ2 protein (magenta) correlate closely throughout
866 embryogenesis. The morphology of the anterior neuroectoderm is visualized with DAPI staining (blue, right
867 column). Some differences between EGFP and Tc-FoxQ2 expression are observed, which may be due to
868 either different dynamics of maturation and degradation of these proteins or to divergence of the
869 enhancer trap signal from the endogenous expression. (A-A''') At NS3, *Tc-foxQ2* expression shows two
870 bilateral domains within the anterior median region. (B-F''') Later, the expression domains split into a
871 stomodeal (asterisk), a median (white arrowhead) and lateral domain (open arrowhead). At NS15, two
872 clusters of cells are observed: The large *anterior-median-foxQ2-cluster* (white arrowhead in F') and a
873 smaller *anterior-lateral-foxQ2-lineage* (open arrowhead in F').

874

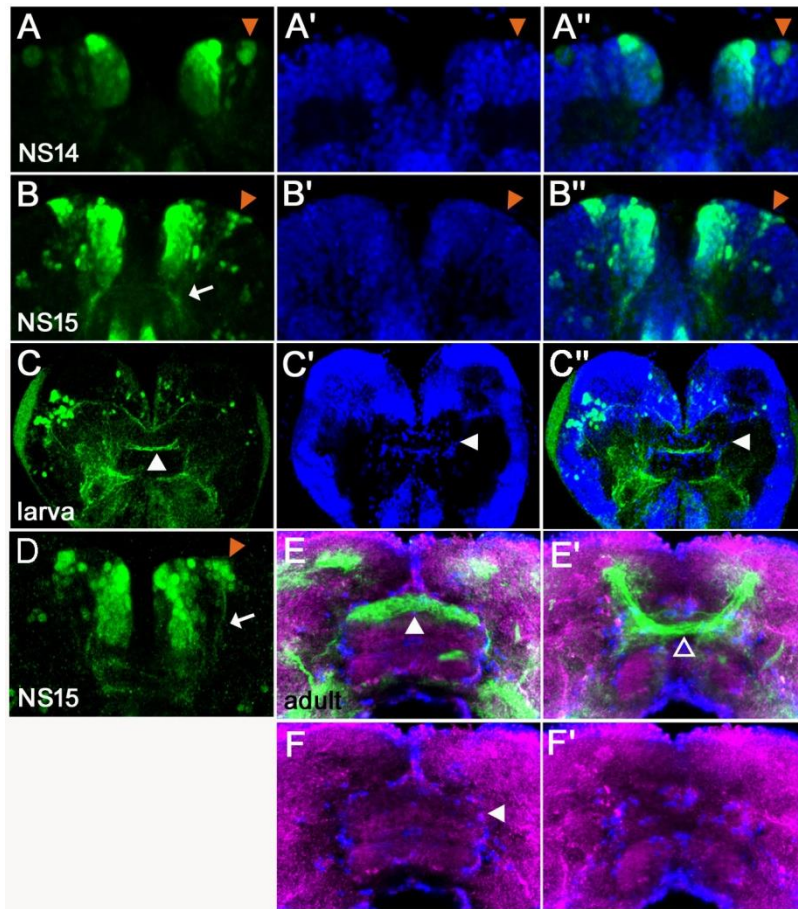


875

876 **Fig. 4. Anterior-media-foxQ2-cluster contributes to the central brain primordium.** Double-
877 immunohistochemistry visualizes the EGFP (green) derived from the *foxQ2-5'-line* and acTub (magenta)
878 which marks axonal projections – neuraxis anterior is up. (A-A') At NS13, the first brain commissure marked
879 by acTub appears (white arrowhead in A'). The cell bodies of the *anterior-median-foxQ2-cluster* are located
880 around this commissure but do not yet project into it. A few weakly stained cells closely attached to the
881 commissure are not Tc-FoxQ2 protein positive (asterisk in A'). (B-B') At NS14, projections within the brain
882 commissure become visible but have not yet reached the midline (white arrowhead in B). One Tc-FoxQ2
883 positive NPC is recognized by its morphology and position (hatched circle in B'). (B) and (B') are not the
884 same embryo but from the same developmental stage. (C-E) At NS15, at least three brain commissures are
885 marked by the *anterior-median-foxQ2-cluster*: One in the circumesophageal commissure (white
886 arrowhead in E), and two commissures within the central brain primordium (white arrowheads in D). The
887 *anterior-median-foxQ2-cluster* produces more cells at this stage. (C'-E') acTub marked brain commissures
888 expand into many fascicles and increase in size. 6-7 axon bundles emanating from the *anterior-median-*
889 *foxQ2-cluster* separately join this midline brain primordium (one of them marked by an arrow in C').

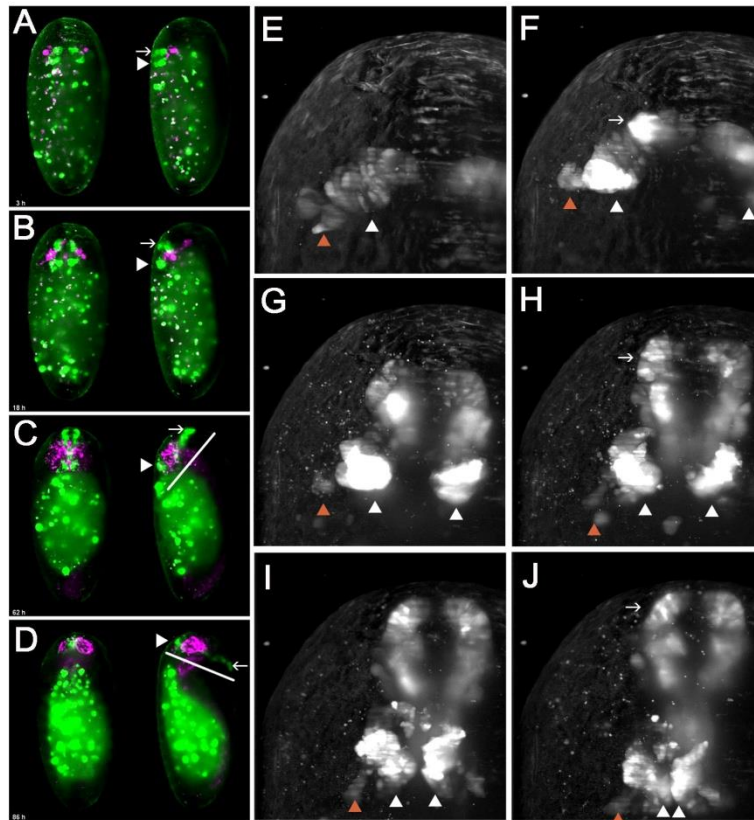
890

891



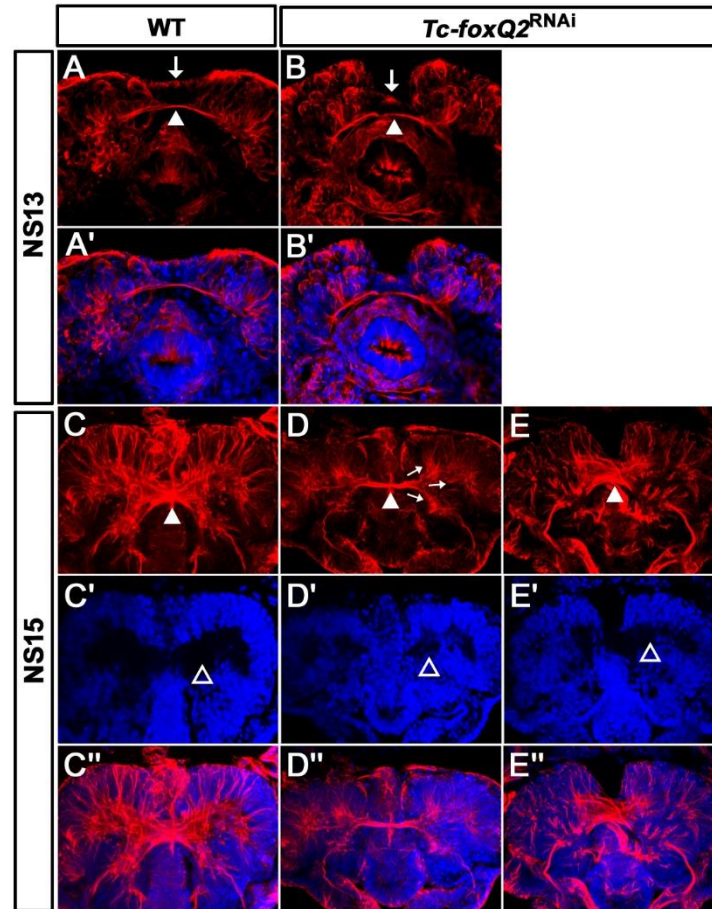
892

893 **Fig. 5. *Tc-foxQ2* positive cells project through the central brain primordium and contribute to the central**
894 **complex.** Immunohistochemistry visualizes EGFP (green) derived from the *foxQ2-5'-line*. Synapsin
895 visualizes adult brain morphology (magenta in E,F) while nuclei are visualized by DAPI (blue in A'-C'). (A-
896 A'') At NS14, the *anterior-lateral-foxQ2-cluster* consists of one NPC and a small number of progeny (orange
897 arrowheads). (B-B'', D) At NS15, more cells are marked by EGFP (orange arrowheads) and their projections
898 join a *Tc-foxQ2* positive axon bundle (white arrows in B, D). (C-C'') EGFP marked projections contribute
899 to the central body in L5 larval brain, which is visualized by its surrounding glia cells (white arrowhead in C').
900 (E-F) EGFP marked projections contribute to the upper unit of the central body in the adult brain (white
901 arrowheads in E) visualized by synapsin and surrounding glia (white arrowhead in F). (E'-F') Another
902 fascicle projects across the midline directly posterior of the central body (open arrowhead).



903

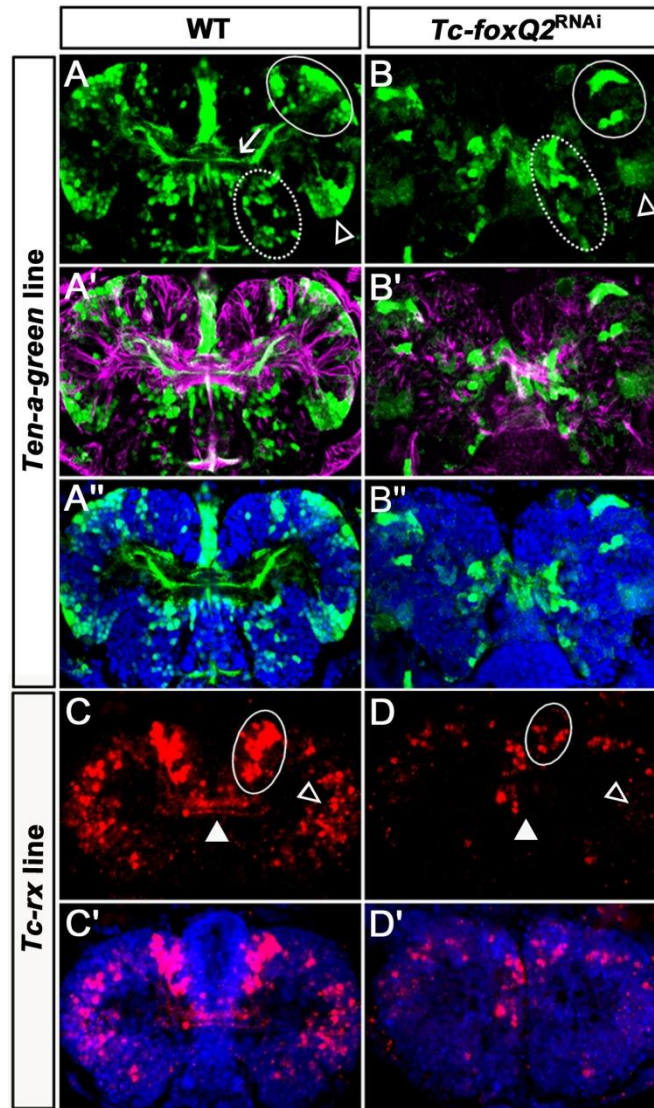
904 **Fig. 6. In vivo imaging reveals morphogenetic movements during brain development.** A cross of the
905 *foxQ2-5'-line* (green) with the *AGOC #6* glia reporter line (magenta) was imaged. (A) EGFP signals in brain
906 and stomodeum start out at the dorsal side (white arrowhead and white arrow, respectively). (B-C) Later,
907 the stomodeum becomes elongated and bends away towards the ventral side. (C-D) An overall ventral
908 bending of the head and brain follows, where the relative positions within the head remain similar
909 (compare white lines in C and D). (E-J) At the same time, the bilateral *Tc-foxQ2* positive cell clusters
910 approach each other towards the midline (white arrowheads). Both the *anterior-median-foxQ2-cluster*
911 (white arrowheads in E-J) and the *lateral-foxQ2-lineage* (orange arrowheads in E-J) can be distinguished
912 throughout development. Note that a small group of marked cells detach from the cluster and fuse at the
913 midline. However, these cells are not Tc-FoxQ2 positive and are, hence, not further considered.



914

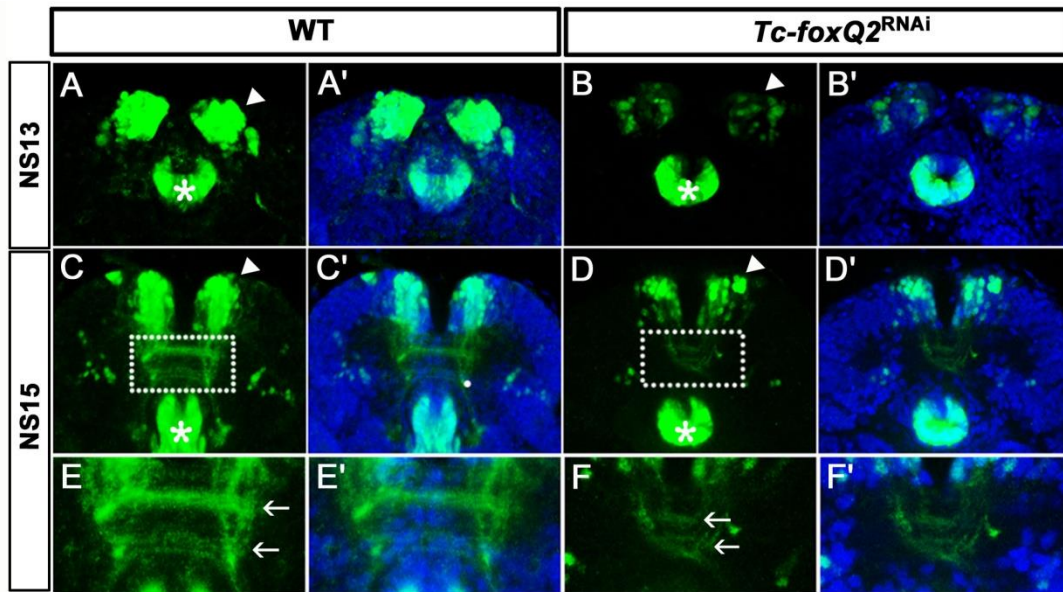
915 **Fig. 7. Loss of *Tc-foxQ2* function leads to arrest of development of brain midline structures in the**
916 **embryo.** Axonal projections are marked by aTub (red) and cell bodies are visualized by DAPI (blue). (A, A')
917 In WT, the primary brain commissure forms at NS13 (white arrowhead in A). (B, B') In RNAi embryos, the
918 primary brain commissure is slightly irregular (white arrowhead in B). The anterior epidermal aberrations
919 reflect the loss of the labrum (compare white arrows in A and B; Kitzmann et al., 2017). (C-C'') In WT NS15
920 embryo, the central brain primordium increases in size and contains more fascicles, some of which form
921 chiasmata at the midline (white arrowhead in C). (D-D'') In strong phenotypes, the primary commissure
922 remains detectable along with three main branches (arrows in D). However, the structures do not expand
923 and commissure splitting does not occur. At the same time, the brain neuropil volume is strongly reduced
924 (compare black space between the cell bodies in C' and D', open arrowheads (arrows in D)). (E-E''). Weak
925 phenotypes show some degree of splitting of the brain commissure but axonal projections are disarranged
926 (white arrowhead in E).

927



928

929 **Fig. 8. Loss of *Tc-foxQ2* function in novel imaging lines confirms the phenotype.** (A-A'') In WT *Ten-a-green*
930 embryos, three groups of cells are marked by EGFP: An anterior group (white circle), a posterior-lateral
931 group (open arrowhead) and a posterior-median group (dashed circle). The central brain primordium is
932 marked with a *Ten-a* positive fascicle projecting across the midline (white arrow in A). (B-B'') In *Tc-foxQ2*
933 RNAi, the *Ten-a* positive projections and the number of the marked cells is reduced (n=4). (C-C') In WT *Tc-*
934 *rx-5'-up* line, the anterior median group of cells marked by DsRed project into the central brain (white
935 circle and white arrowhead). (D-D') In *Tc-foxQ2* RNAi, the cell number in the anterior median group is
936 strongly reduced (n=4; white circle) and the marked brain commissures are absent (white arrowhead). The
937 peripheral cells are reduced in number as well (n=4; compare open arrowheads in C,D).



938

939 **Fig. 9. RNAi in the *foxQ2-5'-line* indicates self-regulation.** (A-B') At NS13, *Tc-foxQ2* RNAi shows the
940 strongly reduced number of marked cells in the *anterior-median-foxQ2-cluster* (n=4; white arrowheads)
941 while the signal in the stomodeum appears to be unaffected (stars). (C-F') In *Tc-foxQ2* RNAi, the number
942 of marked cells decreased significantly (n=4; white arrowhead). The fascicles are reduced and follow an
943 abnormal rounded path instead of the straight line in WT (compare white arrows in E and F).

944

945

946

947

948

949

950

951

952

953

954

955

956